View metadata, citation and similar papers at core.ac.uk
brought to you by CORE
provided by CERN Document Server

Lattice measurements

J. Wenninger
CERN, Geneva, Switzerland

Abstract

The measurement and correction of the main lattice parameters known as the dispersion and Twiss parameters (phase advance and betatron function) is essential for any modern accelerator. Three techniques for optics reconstruction will be presented in this document. A first technique is a simple and direct method based on the strength modulation of individual quadrupoles. A second technique is based on beam position response measurements and is widely used nowadays because it is simple and only requires a good beam position measurement system. Finally, phase advance measurements from multiturn beam position data that provide an easy means for a direct reconstruction of the Twiss parameters will be discussed.

1 Introduction

A good knowledge of the linear machine model is important for accelerator operation since significant optics errors may induce important performance degradations. Measurement and correction of the beam optics is still an active field of development in accelerator physics, as can be seen from the year of publication of the references cited in this document. With the advent of powerful PCs, both in terms of CPU and of memory, it is nowadays possible to tackle numerically complex optics fits that could not be handled in the early 1990s. Advances in beam instrumentation in the past 15 years, both in sensitivity, functionality and accuracy, also provided new opportunities for characterizing and correcting the optics of modern accelerators.

The first section of the document will discuss the measurement of the dispersion function that does not represent a significant difficulty.

Three basic methods exist today to determine the phase advance and the betatron function in an accelerator, with of course many local lab-specific variations. A first method consists in changing the strength of quadrupoles in a controlled way to determine the local betatron function. This *K-modulation* technique is the simplest method to determine the local betatron function within a quadrupole (Section 3). With the advent of more powerful computers in the 1990s, CPU and memory intensive *response methods* became very popular (Section 4). Response techniques have been used worldwide to characterize the optics in rings and in transfer lines. The development and widespread use of *turn-by-turn acquisition* of beam position monitor (BPM) data in the 1990s opened the possibility for direct measurements of the betatron phase advance between BPMs (Section 5).

The optics in transfer lines and the optics matching between a ring and an injection or extraction transfer line may be reconstructed from two-dimensional beam profile measurements based on screens. This method will not be discussed in this document.

2 Dispersion measurement

The dispersion function $D_u(s)$ defines the local sensitivity of the beam trajectory or orbit $u(s)$ to a relative energy error $\Delta p/p$:

$$D_u(s) = \frac{\Delta u_(s)}{\Delta p/p} \, . \tag{1}$$

Non-zero dispersion is produced by bending magnets (or any dipole kick):

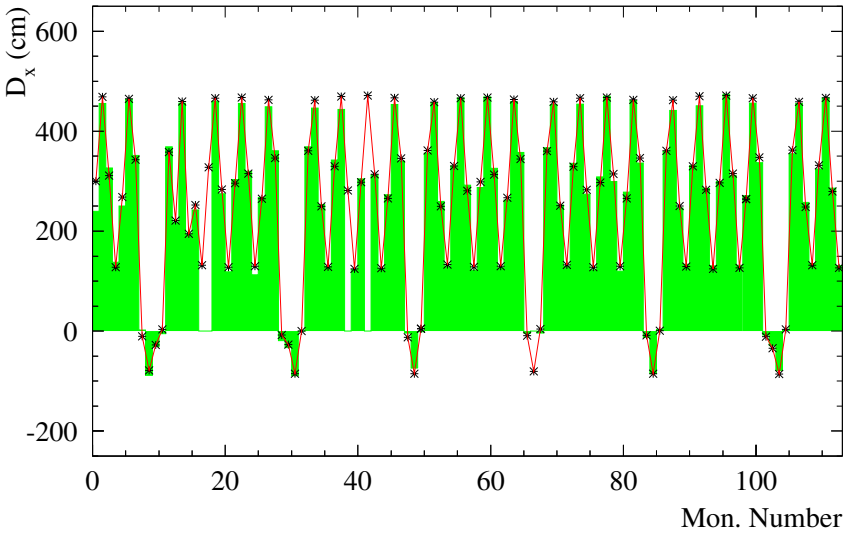

Fig. 1: Horizontal dispersion measurement at the CERN SPS ring from Ref. [1]. The histogram respresent the dispersion measured at the BPMs while the model corresponds to the line and the stars. The SPS has a regular $90°$ lattice with six long straight sections where the dispersion is matched to smaller values.

- A perfectly straight transfer line (linear accelerator) has $D_x = D_y = 0$.
- For an ideal planar ring, $D_x \neq 0$, $D_y = 0$.
- In a real planar ring or transfer line, non-zero vertical dispersion may be produced by coupling or by vertical misalignments of the accelerator elements, in particular quadrupoles. This applies also to linear accelerators.

The dispersion function is the lattice parameter that is easiest to measure. Based on its definition, the dispersion can be obtained from beam position measurements (for both orbit or trajectory) performed for different values of $\Delta p/p$. The dispersion measured at those discrete points can be compared to the model, extrapolated to intermediate position, or corrected using an adequate algorithm. In a ring the simplest way to induce an energy change is to change the RF frequency f_{RF} which induces an energy shift of

$$\frac{\Delta p}{p} = -\left(\alpha_c - \frac{1}{\gamma^2}\right)^{-1} \frac{\Delta f_{\mathrm{RF}}}{f_{\mathrm{RF}}} \tag{2}$$

where $\alpha_c = \gamma_{tr}^{-2}$ is the momentum compaction factor, and $\gamma = E/m_0$ is the relativistic gamma factor. Here γ_{tr} is the value of γ at the transition energy. For synchrotron light sources, the factor $1/\gamma^2$ can normally be neglected. This is usually not the case for protons, except at very high energy (like the LHC) where γ is very large, $\gamma \geq 1000$. An example of a dispersion measurement is shown in Fig. 1 for the CERN SPS ring.

In a transfer line the dispersion depends on the initial condition at the start of the line. The initial conditions include the betatron function β and its derivative $\alpha = -(1/2)d\beta/ds$ as well as the dispersion and its derivative $D' = dD/ds$. In case the model and measurement do not agree, this may be due to an error on the initial conditions or to an error within the transfer line. When the error is due to the initial conditions, it is possible to perform a simple fit to deduce the errors on the initial conditions. Under those assumptions the dispersion error $\Delta D(s)$ between the measurement and the model in the transfer line follows a simple betatron oscillation and can be expressed as

$$\frac{\Delta D(s)}{\sqrt{\beta(s)}} = \left(\frac{\alpha_0\ \Delta D_0}{\sqrt{\beta_0}} + \sqrt{\beta_0}\ \Delta D_0'\right) \sin\mu(s) + \frac{\Delta D_0}{\sqrt{\beta_0}} \cos\mu(s) \tag{3}$$

$$= C \sin(\mu(s) + \phi) \ , \tag{4}$$

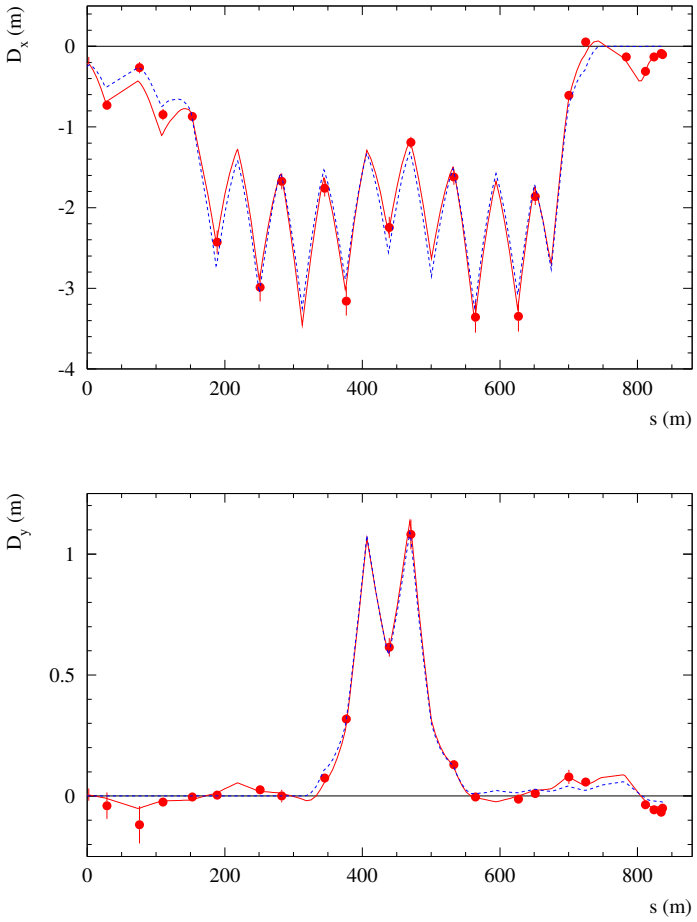

Fig. 2: Dispersion measurement of the CERN Neutrino to Gran Sasso (CNGS) 400 GeV/c transfer line. The horizontal (top) and vertical dispersion (bottom) is shown as a function of the distance along the line. The points correspond to the measurements at the BPMs. The blue line is the nominal dispersion, the red line a fit to the measured dispersion using Eq. (3).

where the constants ΔD_0 and $\Delta D'_0$ are the errors on the initial dispersion and dispersion derivative. Here β, μ, and α refer to the usual Twiss parameters. Index '0' refers to the start of the line ($s = 0$). The constant C is useful to estimate the maximum possible dispersion error at a given point, namely $\Delta D_{\max}(s) = C\sqrt{\beta(s)}$. In practice it is necessary to measure the dispersion, subtract the model expectation, normalize the difference by $\sqrt{\beta}$ [Eq. (3)] and fit the result with a sine function. Figure 2 shows an example of a dispersion measurement at a CERN high-energy transfer line together with a fit of the dispersion error at the entrance of the line. The fit significantly improves the agreement between model and data.

3 Quadrupole strength modulation

When the strength K of a selected quadrupole is changed by a small amount ΔK, the associated tune change ΔQ is proportional to the strength change and to the local betatron function

$$\Delta Q = \frac{1}{4\pi}\int_{s_0}^{s_0+L} \Delta K\beta(s)ds \simeq \frac{\Delta K\bar{\beta}L}{4\pi} \ , \tag{5}$$

where β is the betatron function. Here s_0 is the longitudinal position of the quadrupole, L is the quadrupole length, and $\bar{\beta}$ is the average betatron function over the length of the quadrupole. Equation (5) may be used to determine the average betatron function for a ring provided that:

- The selected quadrupole is individually powered.
- The strength change ΔK is sufficiently well known. This requires an accurate magnet transfer function. It is important that the strength change remains small ($\Delta K/K \leq 1\%$). For large changes β may change by a considerable amount, thus biasing the measurement or making the reconstruction of β more difficult.
- The tune can be measured with high accuracy, for example with a Phase Locked Loop (PLL).

An example for such measurements can be found in Ref. [2].

An elegant measurement technique consists in modulating the strength in time at a frequency f,

$$\Delta K(t) = \Delta K_0 \sin(2\pi f t) \ , \tag{6}$$

and detecting the frequency of the oscillation. In that case multiple magnets can be measured at the same time provided the magnets are modulated at different frequencies and the modulation remains very small, since each modulated quadrupole induces an error on the betatron function at the other quadrupoles. Such a technique was employed at LEP to determine the offset of the BPMs with respect to the nearby quadrupoles, but it was also used to evaluate the possibility of reconstructing the betatron function [3].

The K-modulation technique is frequently used to determine the betatron function β^* at a collision point, which is an important parameter for a collider. Since no quadrupole is installed at the collision point, β^* is obtained from a modulation of the strength of the quadrupoles adjacent to the collision point which is separated from the collision point by a drift space. The betatron function inside the adjacent quadrupole β_Q is related to β^* by

$$\beta_Q = \beta^* + \frac{\Delta s^2}{\beta^*} \ , \tag{7}$$

where Δs is the distance from the collision point to the quadrupole. It is thus possible to deduce the value of β^* from β_Q.

4 Orbit response analysis

The analysis of the machine optics in terms of position response is based on the relation between the beam position measured at the location of N beam position monitors (BPM) represented by a vector $\vec{u}$

$$\vec{u} = \begin{pmatrix} u_1 \\ u_2 \\ \ldots \\ u_N \end{pmatrix} \ , \tag{8}$$

and a set of M dipole magnets (correctors) deflections (kicks) represented by a vector $\vec{\theta}$

$$\vec{\theta} = \begin{pmatrix} \theta_1 \\ \theta_2 \\ \ldots \\ \theta_M \end{pmatrix} \ . \tag{9}$$

Orbit position and corrector deflections are related by the response matrix $\mathbf{R}$ (dimension $N \times M$),

$$\vec{u} = \mathbf{R}\vec{\theta} \, . \tag{10}$$

Element R_{ij} of the response matrix corresponds to the position shift at the i-th monitor due to a unit kick from the j-th corrector. For a linear optics the matrix $\mathbf{R}$ is independent of the kick strength and orbit amplitude, and the element R_{ij} is given for a closed orbit by

$$R_{ij} = \frac{\sqrt{\beta_i \beta_j}\cos(|\mu_i - \mu_j| - \pi Q)}{2\sin(\pi Q)} \quad , \tag{11}$$

and for a trajectory by

$$\begin{aligned} R_{ij} = \sqrt{\beta_i \beta_j}\sin(\mu_i - \mu_j) \quad \mu_i \geq \mu_j \\ R_{ij} = 0 \quad \mu_i < \mu_j \quad , \end{aligned} \tag{12}$$

Q is the machine tune. Matrix $\mathbf{R}$ contains a lot of information about the machine optics, but in a highly entangled form. A measurement of $\mathbf{R}$ does not provide the value of β or μ directly: they must be obtained through a fit that will be discussed in the next section. On the other hand, $\mathbf{R}$ can be determined easily and in a non-destructive way.

The LOCO program [4] is a good example of a popular fit program that is designed to match a measured orbit response matrix of a ring or line with the machine model while properly taking into account the monitors and orbit corrector calibration errors. LOCO was written by J. Safranek in the early 1990s and is now used in many places. While the initial version was written in FORTRAN, there are now Mathlab versions available. Reference [5] provides an excellent overview of the status and use of LOCO.

4.1 LOCO analysis principle

To use the information contained in the response matrix, the first step consists in building the vector $\vec{V}$ obtained by the difference between the measured and the modelled response matrix. The elements of this vector are

$$V_k = \frac{R_{ij}^{\text{meas}} - R_{ij}^{\text{mod}}}{\sigma_i} \qquad \forall i, j \tag{13}$$

where σ_i is the measurement noise of the i^{th} monitor. The norm of vector $\vec{V}$ represents the normalized error of the machine model with respect to the measurement. The goal of the fit is to minimize the difference between model and measurement through the norm of vector $\vec{V}$

$$\|\vec{V}\|^2 = \sum_{k=1}^{N} V_k^2 = \text{minimum} \, , \tag{14}$$

by adjusting N_f fit parameters related to the machine model, to the monitors and to the orbit correctors. For errors distributed according to a Gaussian probability distribution, $\|\vec{V}\|^2$ should be distributed according to a χ^2 distribution. The expected minimum value for $\|\vec{V}\|^2$ is given roughly by the number of elements of $\vec{V}$ minus the number of fit parameters. The value of the minimum provides a statistical test of the fit quality and of the correct assessment of the BPM errors.

To perform a fit of the response, N_f parameters c_l must be selected, and the dependence of each element of vector $\vec{V}$ on each parameter c_l must be evaluated. The resulting sensitivity matrix $\mathbf{S}$ with elements S_{kl} defined by

$$S_{kl} = \frac{\partial V_k}{\partial c_l} \tag{15}$$

can be used to approach the solution by linearizing the problem. The three main parameter classes are:

– BPM calibration factors, where $S_{kl} = -R_{ij}^{\text{mod}}/\sigma_i$.

– Corrector calibration factors, where $S_{kl} = R_{ij}^{\rm mod}/\sigma_i$.
– Optics model parameters (magnetic strengths, element misalignments, etc). For such parameters, the sensitivity must be evaluated with a modelling program like MAD [6] using a linear approximation

$$S_{kl} = \frac{R_{ij}^{\rm mod}(c_l + \delta c_l) - R_{ij}^{\rm mod}(c_l)}{\delta c_l \ \sigma_i} \tag{16}$$

where the response matrix change must be evaluated for an increment δc_l of each parameter.

The norm of vector $\vec{V}$ is minimized iteratively by solving the linear equation

$$\vec{V} + \mathbf{S}\Delta\vec{c} = 0 \tag{17}$$

for the increment $\Delta\vec{c}$ in the parameter vector $\vec{c}$. This equation may be solved using a least-squares solver. Once a new parameter vector $\vec{c} + \Delta\vec{c}$ is obtained, the procedure is iterated and the model and vector $\vec{V}$ updated. In particular, the sensitivity matrix [Eq. (15)] must be re-evaluated around the new optimum and Eq. (17) must be solved again. This procedure is iterated until a stable solution is found, i.e., when $\Delta\vec{c} \simeq 0$.

It is important to note that matrix $\mathbf{S}$ may be rank deficient (singular): there are, for example, an infinite number of solutions obtained by multiplying both the orbit corrector strength and the orbit change by the same scale factor. For this reason it is not possible to determine the absolute calibration of orbit monitors or corrector magnets from the response matrix alone. For the horizontal plane, the absolute scale can be obtained by a known energy change over the RF frequency. The radial movement can be used to calibrate the absolute scale of the horizontal monitors.

Equation (17) is solved using the Singular Value Decomposition algorithm [7]. For a matrix $\mathbf{S}$ of dimension $n \times m$ with $n \geq m$ the singular value decomposition has the form

$$\mathbf{S} = \mathbf{U}\mathbf{W}\mathbf{V}^{\mathbf{T}} = \mathbf{U} \begin{pmatrix} w_1 & 0 & ... & 0 \\ 0 & w_2 & & \\ ... & & ... & 0 \\ 0 & ... & 0 & w_m \end{pmatrix} \mathbf{V}^{\mathbf{T}} \,, \tag{18}$$

where $\mathbf{W}$ is a diagonal $m \times m$ matrix with non-negative diagonal elements. Here $\mathbf{V}^{\mathbf{T}}$ is the transpose of the $m \times m$ orthogonal matrix $\mathbf{V}$,

$$\mathbf{V}\mathbf{V}^{\mathbf{T}} = \mathbf{V}^{\mathbf{T}}\mathbf{V} = \mathbf{I} \,, \tag{19}$$

while $\mathbf{U}$ is an $n \times m$ column-orthogonal matrix

$$\mathbf{U}^{\mathbf{T}}\mathbf{U} = \mathbf{I} \,. \tag{20}$$

The least-squares solution to Eq. (17) is

$$\Delta\vec{c} = \mathbf{V}\mathbf{W}^{-1}\mathbf{U}^{T} \ \vec{V} \tag{21}$$

where $\mathbf{W}^{-1}$ is the 'inverse' of matrix $\mathbf{W}$, with all singular elements $1/w_k > 1/\epsilon$ set to 0. Here $\epsilon > 0$ is a selected cut-off value that can be adapted for each data set depending in particular on input conditions (noise, etc).

For a machine with N BPMs and M corrector magnets *per plane*, the size of matrix $\mathbf{S}$ is

– $(2 \times N \times M) \times (2 \times (N + M) + N_f)$ if the coupling terms between the planes are ignored,
– $(4 \times N \times M) \times (2 \times (N + M) + N_f)$ if the coupling terms between the planes are included,

since the number of parameters must a priori include the calibration factors of all BPMs and correctors $[2 \times (N + M)]$. For the LHC, $N \cong 500$ and $M \cong 280$, and $\mathbf{S}$ has dimensions $\sim 280\,000 \times 1\,600$. It is basically impossible to handle matrices of the size required for the LHC. For such a case the data can of course be split into smaller data sets by using only a subset of the orbit correctors. For the LHC 20–50 orbit correctors ($\approx 10\%$ of the total) are sufficient to probe all phases.

4.2 Response data examples

An example for response data fits is shown in Fig. 3 for the CERN SPS ring. The raw data shows large deviations between data and model that are mostly due to a large difference between the model tune and the actual tune of the machine. The tune error was introduced on purpose to test the convergence of the fit. Many other examples for applications of response fits can be found in Ref. [5].

The response fits can also be used in transfer lines or linear accelerators, an example is shown in Fig. 4 for a 450 GeV/c proton injection transfer line to the LHC ring. In this case the response measurement indicated a 'spectacular' error in the optics. From the fit to the response data it was possible to trace down the error to a 20% gradient error of one of the quadrupoles that was due to an error in the current setting of the power converter.

Response fits have been used successfully in all injection and extraction transfer lines of the SPS [8]. For the long SPS lines (1 to 3 km) the response data is very sensitive to focusing errors. Phase advance errors of 0.3 to 1% could be identified and corrected for the main lattice cells of the transfer lines.

There is, however, an important point to note for transfer lines: the response data is only sensitive to optics errors that have their origin inside the transfer line, but the betatron function (and therefore the beam profile) in the line depends on the initial conditions at the start of the line. It is therefore possible that while the response measurement agree perfectly with the model, the beam envelope can exhibit very large errors due to incorrect initial conditions.

4.3 Alternative fit techniques

An alternative fit method for response data has been used successfully at KEKB [9], and will also be used for the LHC. From Eq. (11) the orbit shift Δu_{ij} at monitor i due to a kick $\Delta\theta_j$ at corrector j may be rewritten as

$$\Delta u_{ij} = \left(\cos(\pi Q) f_j X_j^C - S_{ij}\sin(\pi Q) f_j Y_j^C\right) X_i^M + \left(\cos(\pi Q) f_j Y_j^C + S_{ij}\sin(\pi Q) f_j X_j^C\right) Y_i^M \quad (22)$$

where

$$f_j = \frac{\Delta\theta_j}{2\sin(\pi Q)} \qquad S_{ij} = \mathrm{sign}(\mu_i - \mu_j) \quad (23)$$

and

$$X_i^l = \sqrt{\beta_i^l}\cos(\mu_i^l) \qquad Y_i^l = \sqrt{\beta_i^l}\sin(\mu_i^l)\ . \quad (24)$$

The index l refers to either the monitors (M) or to the correctors (C). If the measured orbit displacement is denoted by $\Delta\bar{u}_{ij}$, the residual error between measured displacement and model is

$$\chi^2 = \sum_{i,j}(\Delta\bar{u}_{ij} - \Delta u_{ij})^2\ . \quad (25)$$

This last equation corresponds to a quadratic equation in either the set of monitor $\{X_i^M, Y_i^M\}$ or corrector $\{X_i^C, Y_i^C\}$ parameters which may be solved by alternating least-squares inversions for either monitor or corrector parameters. In a first step the initial values given by the model are, for example, inserted for $\{X_i^M, Y_i^M\}$ and the equation is solved by $\{X_i^C, Y_i^C\}$. In the next step new $\{X_i^M, Y_i^M\}$ are calculated based on the previous solutions for $\{X_i^C, Y_i^C\}$. This procedure is repeated until the solutions are stable.

The resulting $\{X_i^l, Y_i^l\}$ can be used to reconstruct the betatron phases since

$$\tan(\mu_i^l) = \frac{Y_i^l}{X_i^l}\ . \quad (26)$$

It must be noted that the monitor and corrector calibration factors may be ignored because such calibration factors cancel out in the above equation for the phase advance. The result for the phase does not change if both Y_i^l and X_i^l are multiplied by the same factor.

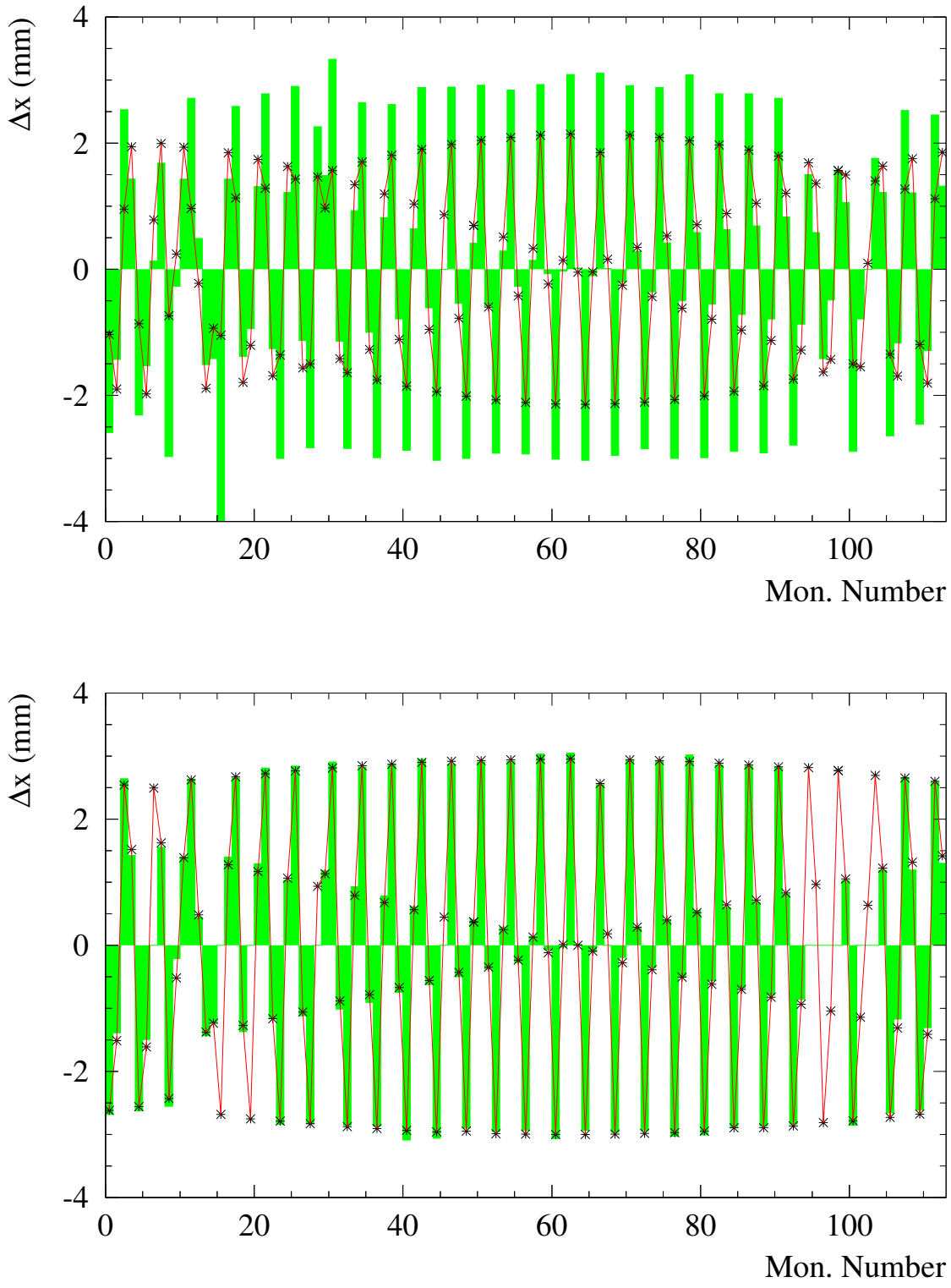

Fig. 3: Example of a response measurement at the CERN SPS ring. The orbit response is shown at all horizontal BPMs for a horizontal orbit corrector before (top) and after (bottom) a fit to the response data for a number of horizontal and vertical correctors. The histogram represents the data, the line and stars the fitted model. The fit parameters include BPM and corrector calibration factors as well as the strength of the main lattice quadrupoles. In this example the large error in the response is due to a difference of the horizontal tune.

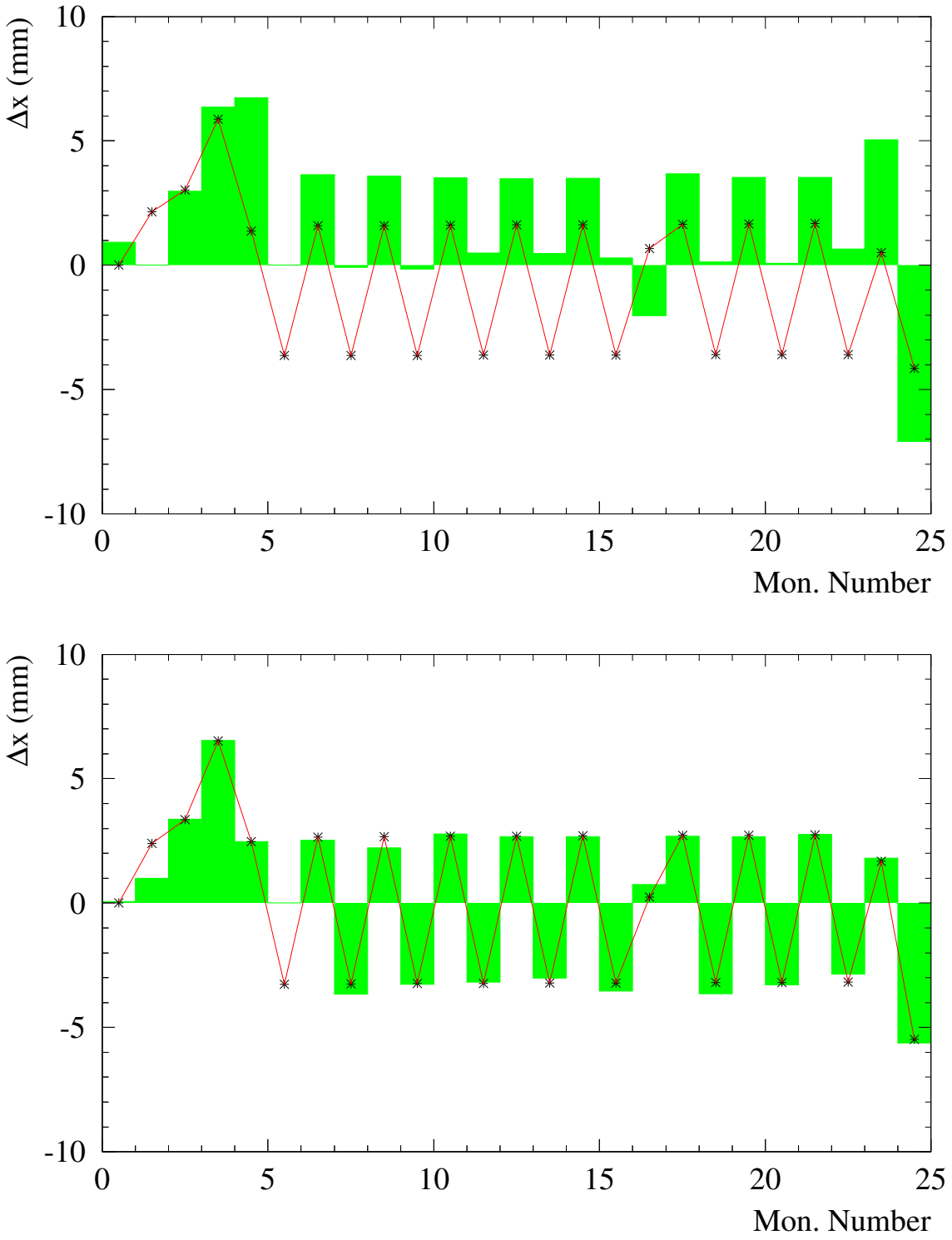

Fig. 4: Example of a response measurement in a 450 GeV/c proton transfer line between the CERN SPS and LHC rings. The trajectory response is shown for the first horizontal steering magnet of the transfer line. The histogram represents the data, the line and stars the fitted model. In the top figure there is a very large discrepancy between the data and the model due to a 20% strength error of one of the first horizontally focusing quadrupoles. After a fit to the response data the error was corrected and data and model agree (bottom).

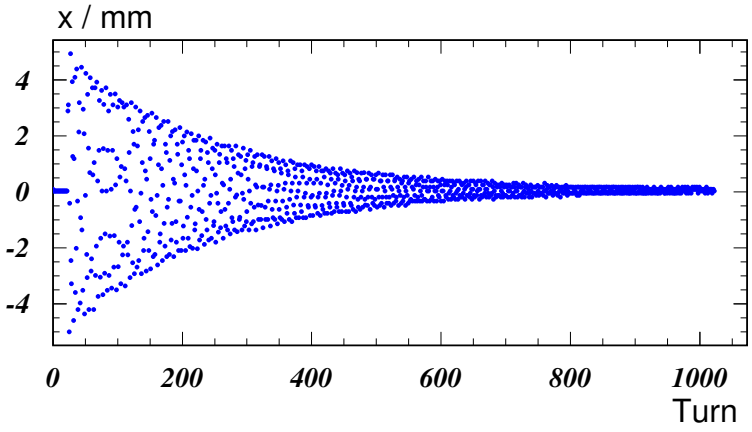

Fig. 5: Example of a turn-by-turn beam position measurement following a kick at LEP

5 Multiturn measurements

In many modern circular accelerators the BPM system is able to record the position of individual bunches or of part of the beam on a turn-by-turn basis (*multiturn* acquisition) [10–12], see, for example, Fig. 5. The betatron oscillation amplitude u ($u = x, y$) of a bunch measured turn by turn in a ring at a BPM number i can be expressed as

$$u_i(k) = A_i(k)\sin(2\pi Qk + \mu_i + \phi)\ , \tag{27}$$

where k labels the turn number $k = 1, N$; A is the amplitude; Q is the tune; μ_i is the phase advance at the BPM; and ϕ is an arbitrary phase factor. Since the difference of the phase factors for two BPMs is nothing but the betatron phase advance $\mu_i - \mu_j$, a measurement of the phase of the oscillation at every BPM provides a *direct measurement of the betatron phase advance*. The phase may be extracted from the multiturn data from a FFT, a harmonic analysis, or any other frequency analysis. It should be noted that in general a simple FFT does not provide sufficient accuracy on the phase [10].

The phase advance may be reconstructed with high accuracy provided

- the betatron oscillation is long enough (damping),
- the turn-by-turn resolution of the BPM measurement is good.

The interest of this method lies in the fact that the results do not depend on the BPM calibration, since only the phase of the oscillation is measured. The amplitude factor A does not affect the result, provided that the amplitude is sufficient as compared to the measurement noise. It must be noted that the phase measurement may be biased when the beam oscillation is damped. The betatron function itself may be reconstructed at any BPM using the measured phase advance to two adjacent BPMs from the following equation [10, 11]:

$$\beta_{2,\text{meas}} = \beta_{2,\text{model}}\frac{\cot(\Delta\mu_{12,\text{meas}}) - \cot(\Delta\mu_{23,\text{meas}})}{\cot(\Delta\mu_{12,\text{model}}) - \cot(\Delta\mu_{23,\text{model}})} \tag{28}$$

where $\Delta\mu_{ij}$ is the phase advance between BPM i and j, see Fig. 6. The subscript meas refers to the measurement, and the subscript model to the nominal model. It is important to note that model information is used to reconstruct β. The value of β is only accurate if there are no significant sources of errors within the region. For large machines with distributed errors this is a good assumption, at the 26.7 km long LEP machine the typical bias on β was at the level of 1% [11]. Figure 7 shows a measurement of $\beta_{\text{meas}}/\beta_{\text{model}}$ for LEP at 45 GeV.

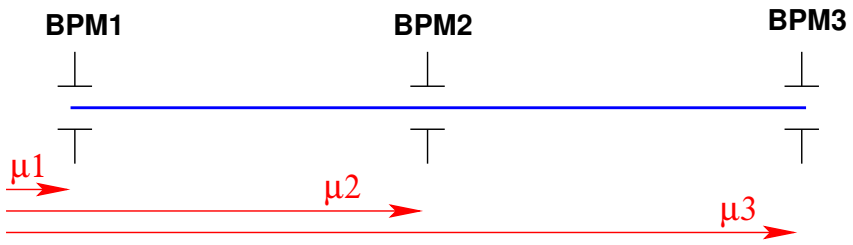

Fig. 6: Layout of the three BPMs used for reconstruction of the betatron function in Eq. (28)

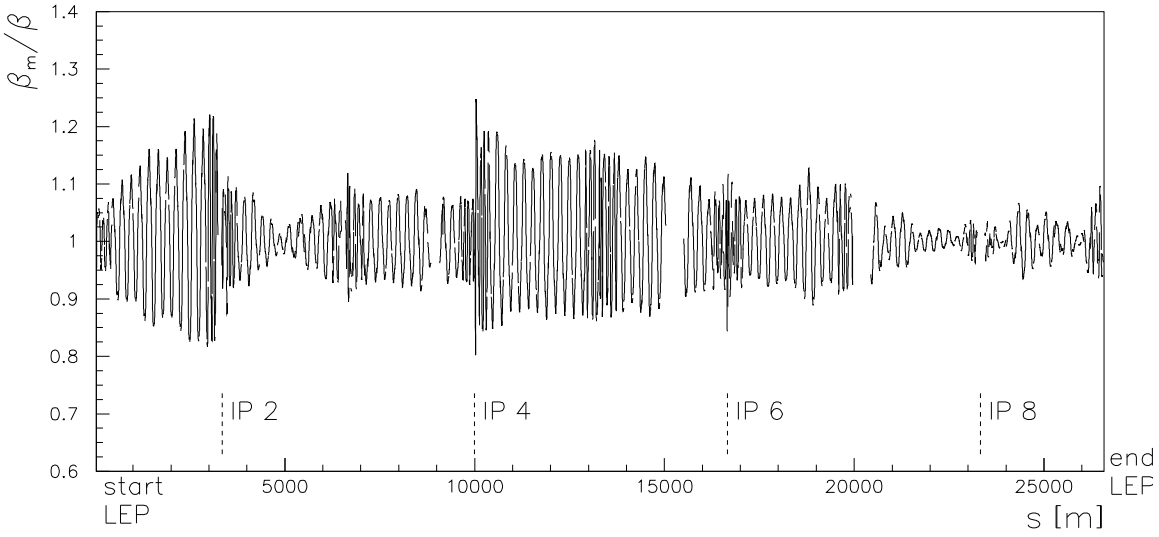

Fig. 7: Beta-beating $\beta_{\text{meas}}/\beta_{\text{model}}$ reconstructed for LEP at 45 GeV/c from a multiturn analysis (courtesy P. Castro). One notes the abrupt changes of the errors in the interaction regions (IPs) due to the low-beta insertion. The peak betatron function error is around 25%.

The measurement error on the betatron function depends on the phase error σ_ϕ and on the phase advance between the BPMs. Assuming that the phase advance between the BPMs is identical, $\Delta\mu_{12} = \Delta\mu_{23} = 0.5\Delta\mu_{13} = \Delta\mu$, then the error on the betatron function reconstruction based on Eq. (28) is

$$\frac{\sigma_\beta}{\beta} = \frac{\sigma_\phi}{\sqrt{2}} \left(\frac{1 + \tan^2 \Delta\mu}{\tan \Delta\mu} \right) \quad . \tag{29}$$

Figure 8 displays the relative error on β as a function of $\Delta\mu$. As the phase advance approaches 90° the error diverges. This effect can be explained from the form of the *beta-beat* wave induced by a gradient error ΔKL at a location s_0. The betatron function error $\Delta\beta(s)$ oscillates at twice the betatron frequency:

$$\frac{\Delta\beta(s)}{\beta(s)} = \beta(s_0) \, \frac{cos(|2(\mu(s) - \mu(s_0))| - \pi Q)}{2\sin(2\pi Q)} \, \Delta KL \quad . \tag{30}$$

For $\Delta\mu$ = 90° the phase advance of the betatron function beating is therefore 180° between the monitors which corresponds to the Nyquist frequency. At this point it is no longer possible to measure the amplitude of the betatron beating.

The reconstructed betatron function may be used in a fit or a matching program to determine correction factors for quadrupole strengths to reduce the beta-beating. It is also possible to perform the same fit directly from the phase advance measurement, which has the advantage of not relying on any model since it is measured directly (and not reconstructed from a model like the betatron function). The phase advance data may be combined with dispersion data to further constrain the machine optics for the

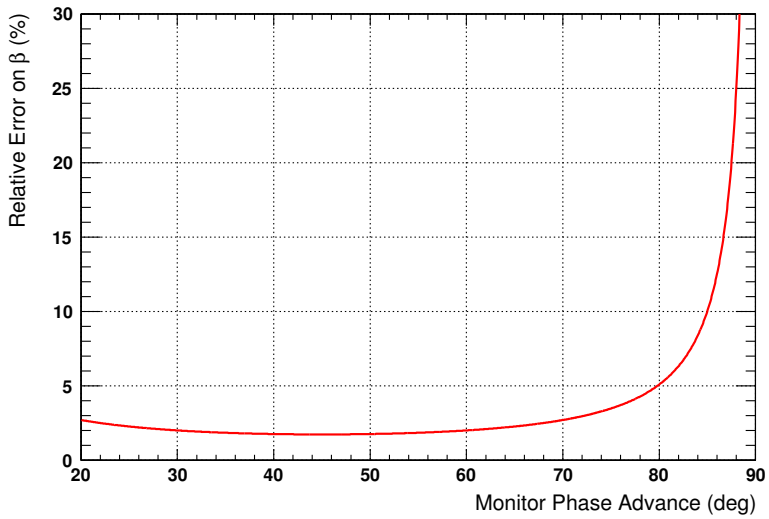

Fig. 8: Betatron function measurement error as a function of the phase advance between adjacent BPMs for an assumed phase measurement error of $0.5°$

fits. It is noteworthy to observe that such fits require significantly fewer free parameters than the response fits, since it is not necessary to handle the calibration factors for BPMs and corrector magnets.

In addition to the uncoupled betatron function and phase advance, multiturn measurements may also be used to reconstruct and correct the coupling between the horizontal and vertical planes [12]. Various techniques have been developed in the past decade to take best advantage of multiturn data, including the analysis of the multiturn data based on the concept of eigenmodes [13]. The multiturn data is placed into a matrix $\mathbf{B}$:

$$B_{ik} = u_i(k) \quad , \tag{31}$$

where $u_i(k)$ is the beam position measured at turn k for monitor number i. Then $\mathbf{B}$ is analysed using SVD (see Section 4) to identify the main eigenmodes. Those can be used to reconstruct coupling and betatron phases.

A very interesting extension of the phase advance measurement is to determine the phase advance changes with respect to the momentum error or to the beam intensity. In the first case the chromatic errors and corrections with the sextupoles may be investigated. In the second case the effects of impedances may be studied, or unknown impedance source may potentially be localized. The chromatic phase advance is defined as the phase advance change with respect to the momentum change

$$\frac{d\mu}{dp/p} \quad . \tag{32}$$

An example of a measurement of the chromatic phase advance is shown in Fig. 9 for LEP [14].

5.1 Beam exciters

The classical method to excite a beam for a multiturn measurement is a fast kicker magnet that provides a short kick to the beam followed by a free oscillation where the beam amplitude is decreasing due to damping from synchrotron radiation or collective effects (for example Landau damping). While such a method is adequate for electron beams or for fast pulsing hadron rings, it is not well adapted to hadron colliders where the beams must be stored with the smallest possible emittance blowup for long time periods.

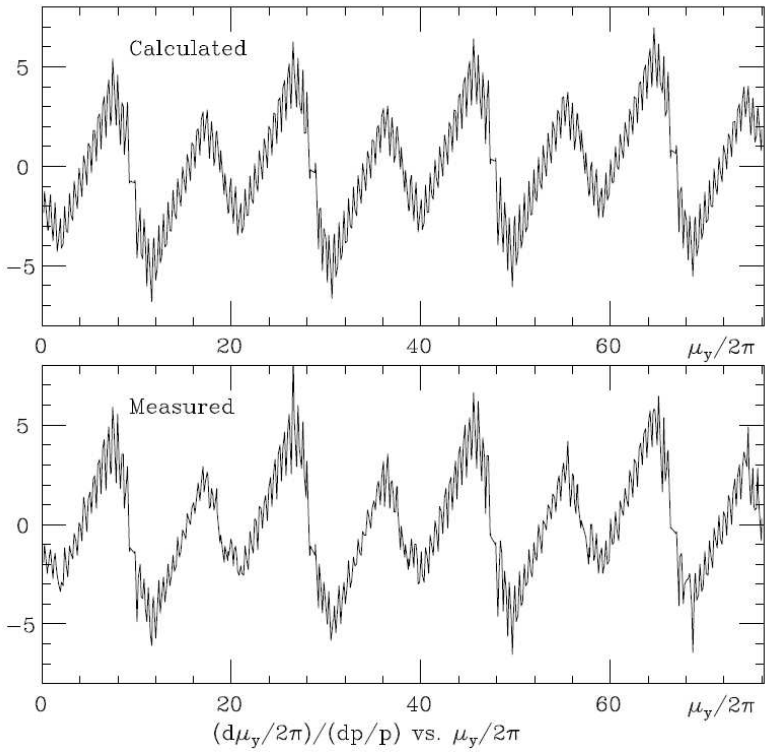

Fig. 9: Measurement of the horizontal chromatic phase advance at LEP (from Ref. [14]). The chromatic phase changes rapidly in the eight straight sections. The errors introduced in the straight sections must be compensated in the arcs.

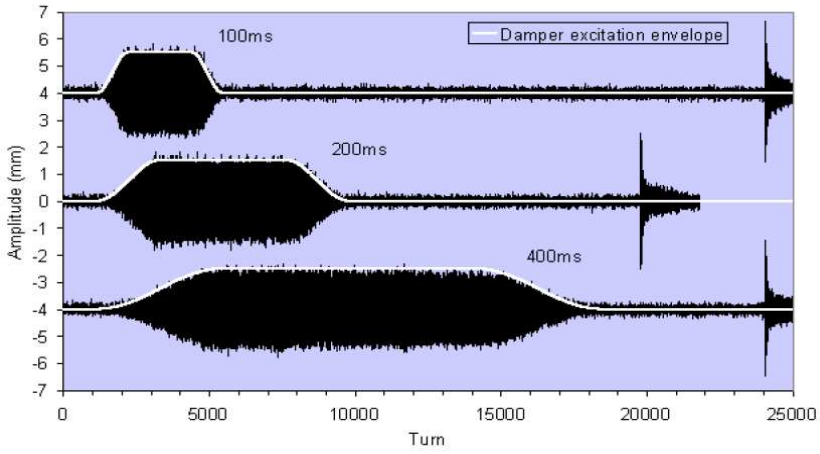

Fig. 10: Example of proton beam oscillations obtained at the SPS based on the AC dipole principle (from Ref. [16])

To overcome this limitation an excitation method based on the so- called *AC dipole* principle has been developed in the last decade [15, 16]. The AC dipole provides a forced oscillation of the beam at a frequency that is close to but not exactly equal to the tune. The distance to the tune line (or to resonances) must be sufficient to avoid emittance blowup. The minimum distance depends on the machine non-linearities and on the chromaticity. The AC dipole is able to provide very long excitations at constant amplitude that provide ideal conditions for multiturn measurements and optics reconstruction for hadron colliders. An example is shown in Fig. 10.

R&D work at CERN is aimed at overcoming the limitations on beam excitations and at providing potentially continuous phase advance measurements. Tests on a continuous phase advance measurement using a high-sensitivity tune measurement device based on the detection of micron-scale natural beam oscillations will be performed in the near future at the SPS. If successful this technique opens the possibility of quasi real-time optics measurements for rings.

6 Summary

Three methods to determine the linear optics have been presented in this document. Each method has its advantages and disadvantages or requires specific instrumentation or machine layout. We summarize here the main points.

- Strength modulation is a very simple method to determine directly the betatron function at a selected quadrupole. Prerequisites are individually powered quadrupoles, a good knowledge of the magnet transfer function, and a precise tune measurement.
- Response measurements can be performed at basically every accelerator, linear or circular, since they only require steering elements and a BPM system. It is simple to apply, but its disadvantage is that it does not provide a direct measurement of any optics parameters like β or μ. To access the quality of the optics it is necessary to perform a complicated fit.
- Multiturn measurements of the beam position provide a direct measurement of the phase advance between BPMs that is independent of the BPM or of the exciter calibration. The betatron function can be reconstructed easily from the phase advance. It requires, however, a sufficiently large or long excitation of the beam and a turn-by-turn acquisition of the beam position.

References

[1] J. Wenninger, *Orbit response measurements at the SPS*, CERN-AB-2004-009.

[2] O. Berrig *et al.*, *Measuring beta- functions with K-modulation*, Proceedings DIPAC 2001, ESRF, Grenoble, France, available at the URL `http://accelconf.web.cern.ch/accelconf/`

[3] B. Dehning *et al.*, *Dynamic beam based calibration of beam position monitors*, Proceedings of the 1998 European Particle Accelerator Conference, Stockholm, Sweden, available at the URL `http://accelconf.web.cern.ch/accelconf/`

[4] J. Safranek, Nucl. Instrum. Methods **A388** (1997) 27.
J. Safranek *et al.*, *Optics characterization and correction at PEP-II*, Proceedings of the 1999 Particle Accelerator Conference, New York, 1999, available at the URL `http://accelconf.web.cern.ch/accelconf/`

[5] ICFA Beam Dynamics Newsletter No. 44, Theme Section LOCO, available at `http://icfa-usa.jlab.org/archive/newsletter.shtml`.

[6] H. Grote and F. Iselin, *The MAD Program*, CERN/SL/90-13 Rev. 5, 1996.

[7] W. Press, B. Flannery, S. Teukolsky and W. Vetterling, *Numerical Recipes* (Cambridge University Press, Cambridge, 1987).

[8] J. Wenninger, *Study of the TI 8 optics and beam stability based on beam trajectories*, AB-Note-2006-021 OP.
J. Wenninger, *Beam stability and optics studies of the CNGS transfer line*, AB-Note-2007-008 OP.
J. Wenninger, *Response matrix and dispersion study of the TI2 transfer line*, CERN-AB-Note-2008-008 OP.

[9] A. Morita *et al.*, *Measurement and correction of on- and off-momentum beta functions at KEKB*, Phys. Rev. ST Accel. Beams **10** (2007) 072801.

[10] P. Castro, *Luminosity and beta function measurement at the electron position collider ring LEP*, CERN Doctoral Thesis, CERN SL/96-70 (BI).

[11] P. Castro, *Applications of the 1000-turns orbit measurement system at LEP*, Proceedings of the 1999 Particle Accelerator Conference, New York, 1999, available at the URL `http://accelconf.web.cern.ch/accelconf/`

[12] D. Sagan *et al.*, *Betatron phase and coupling measurement at the Cornell Electron/Positron Storage Ring*, Phys. Rev. ST Accel. Beams **3** (2000) 092801.
D. Sagan, *Betatron phase and coupling correction at the Cornell Electron/Positron Strorage Ring*, Phys. Rev. ST Accel. Beams **3** (2000) 012801.

[13] C. Wang *et al.*, *Phase advance and β function measurements using model-independent analysis*, Phys. Rev. ST Accel. Beams **6** (2003) 104001.
C. Wang, *Untangling mixed modes in model-independent analysis of beam dynamics in circular accelerators*, Phys. Rev. ST Accel. Beams **7** (2004) 114001.

[14] D. Brandt *et al.*, *Measurement of chromatic effects in LEP*, CERN-SL-95-35 AP.

[15] M. Bai *et al.*, *Experimental test of coherent resonance excitations*, Phys. Rev. **E56** (1997) 6002–7.

[16] O. Berrig *et al.*, *Excitation of large transverse beam oscillations without emittance blow-up using the AC- dipole principle*, Proceedings of DIPAC 2001, ESRF, Grenoble, France, available at the URL `http://accelconf.web.cern.ch/accelconf/`